

Laser Sheet Technique for Visualizing a Periodic Rotor Wake

A. G. Brand,* N. M. Komerath,†
and H. M. McMahon‡

Georgia Institute of Technology, Atlanta, Georgia

Introduction

LASER sheets have been used to illuminate cross sections of steady flowfields for several years. Intense sheets of light only a few millimeters in thickness can be produced by either expanding a single laser beam with a cylindrical lens or by rapidly sweeping the beam by means of a vibrating mirror or other optical device.^{1,2} Generally, smoke or other seed particles which scatter light as they pass through the laser sheet are introduced upstream of the region of interest. Streamlines and vortical structures are identified respectively as streaks and swirl patterns in the illuminated region.^{3,4}

Recent experiments conducted in the John J. Harper 2.31 m \times 2.74 m (7 \times 9 ft) low-speed wind tunnel at the Georgia Institute of Technology employed a strobed laser sheet to visualize the periodic flowfield between a model rotor and an airframe in forward flight. A nonintrusive method was developed to determine accurately tip vortex trajectories in a uniformly seeded flow. Unlike Schlieren, shadowgraphic, or interferometric methods, the laser sheet technique is well-suited for visualizing the incompressible (low Mach number) flows common to rotorcraft. Quantitative data valuable for use in the interpretation of vortex/airframe interaction measurements were gathered using this technique, as reported in Ref. 5. Used in conjunction with laser velocimeter measurements, the laser sheet flow visualization approach provides a powerful means for documenting vortex jitter or other flow instabilities that can affect measurements. The methods described are adaptable to many situations requiring visualization of a periodic flow structure.

Facility Description

The idealized rotorcraft test configuration consisted of a cylindrical (134 mm diam) airframe with a hemispherical nose. It is supported on a sting mount, independent of a two-bladed teetering rotor, which is driven by a shaft projecting down from the wind tunnel ceiling. The rotor radius (R) of 0.45 m and a constant 2100 rpm operating speed results in a tip speed of 100 m/s. Forward flight is simulated by inclining the drive shaft 6 deg upstream and varying the test section velocity. A complete description of the facility, rotor, and airframe instrumentation is given in Ref. 6.

A schematic of the flow visualization setup is shown in Fig. 1. A 5 W argon ion laser is used to create an intense sheet of light, less than 3 mm thick, within the test section. The sheet is rendered visible by particles of atomized mineral oil that reflect and scatter light. The seed particle generator is located downstream of the test section; since the wind tunnel is a closed-return type, these particles remain confined, distributing themselves uniformly throughout the tunnel circuit.

The flow associated with the rotor blade tip vortices creates a seed particle void in the vortex core. When a tip vortex in-

tersects the laser sheet, it can be identified as a dark (unlighted) region. This dark spot contrasts sharply with the bright, uniformly seeded surroundings. Many factors determine the size of the observed particle void, including vortex strength, vortex age, and perhaps particle size. Velocimeter measurements indicate the core diameter to be approximately equal to the observed particle void diameter.⁵

It should be noted that, although a sheet of vorticity shed from the rotor blade trailing edge is also part of the wake structure, such a sheet is not visible if seeding is uniform. The vortex sheet does not provide a mechanism for creating particle voids. Consequently, no contrast with the surrounding flowfield is apparent during intersection of a vortex sheet with a laser sheet. However, vortex sheets have been visualized by careful positioning of the seeder upstream of the rotor. Concentrated filaments of seed particles create nonuniform brightness bands in the light sheet, and a vortex sheet can then be detected as a sudden shift, or discontinuity, in a band of light. Possible flow distortions caused by the wake of the seeder and support, or by the momentum of the seeder jet, detract from the nonintrusiveness of this technique. Thus, for the following results, the seeder was placed downstream of the test configuration, and the emphasis was on the rotor tip vortex.

Experimental Method

In steady forward flight, the rotor wake is periodic. That is, the wake geometry is repeated each 360 deg of blade rotation. Since a rotor with two identical blades is tested here, the wake geometry repeats every 180 deg of rotation. This periodic nature of the rotor wake can be exploited to obtain the rotor wake geometry as a function of blade azimuth angle.

Referring to the flow visualization arrangement shown in Fig. 1, the laser beam is directed to intersect the stationary mirror in the test section by using traversing mirrors located outside the test section. For the present application, the stationary mirror inside the test section aligns the laser beam with a cylindrical lens which expands the beam into a vertical light sheet. The sheet location is predetermined to illuminate any desired cross section of the wake. Secure mirror fixtures within the test section are essential, since small deflections arising from aerodynamic forces can result in beam misalignment with respect to the cylindrical lens.

In order to visually capture the image of the moving vortex core, the laser sheet is strobed at or near the rotor fundamental frequency. The rotor fundamental frequency is 70 Hz, corresponding to a two-bladed rotor operating at 2100 rpm. Since the flowfield due to the rotor is periodic, it is natural to use a strobing technique to "freeze" the vortex images in the light plane. This technique eliminates the need for costly high-speed photographic equipment. Additionally, it allows the experimenter to observe vortex core activity with the naked eye and position cameras to record only the region of interest.

Strobing is accomplished by an acousto-optic modulator system that can periodically deflect the laser beam. While the beam is deflected, it travels along the path that produces the laser sheet. Undeflected, the beam is blocked off and no sheet is produced. The deflection frequency is controlled by a pulse generator so that strobing can be synchronized with the rotor. The duration of laser sheet illumination over one cycle is determined by pulse width. An excessive pulse width will cause blurred images in the light sheet, since a large blade rotation occurs while the sheet is illuminated. In order to produce a crisp image, a short pulse width is desirable. The light sensitivity of the camera must be considered, however, since image intensity is directly affected by pulse width. An unavoidable consequence of strobing the laser sheet is that, for any reasonable pulse width, the sheet intensity is cut drastically.

For the setup shown in Fig. 1, the laser beam is expanded along the top of the airframe beneath the rotor hub. The light sheet opens vertically, allowing cross sections of tip vortices to be observed as they sweep back and descend toward the airframe in forward flight. Moving images of tip vortex cross sec-

Received Oct. 20, 1987; revision received Nov. 5, 1987. Copyright © American Institute of Aeronautics and Astronautics, Inc., 1988. All rights reserved.

*Graduate Research Fellow, School of Aerospace Engineering, Member AIAA.

†Assistant Professor, School of Aerospace Engineering, Member AIAA.

‡Professor, School of Aerospace Engineering, Senior Member of AIAA.

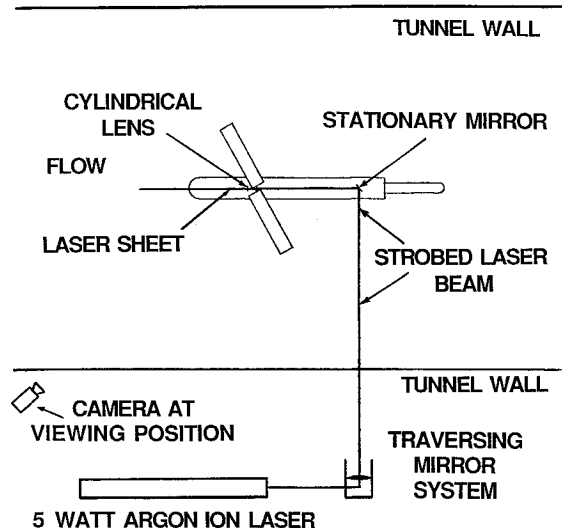


Fig. 1 Flow visualization setup.

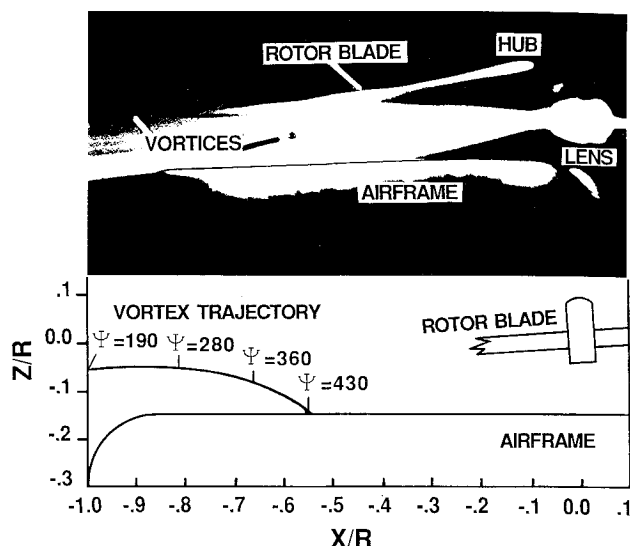


Fig. 2 Vortex trajectory obtained from flow visualization.

tions are obtained by setting the modulator deflection frequency close to, but less than 70 Hz. The rotor blades then appear to advance in the direction of rotation as they penetrate the laser sheet. This approach was used in conjunction with a 7.5 lux professional quality video camera to record and determine vortex trajectories as a function of blade azimuth angle.

Low light conditions require the camera to view the laser sheet from a forward scatter position as shown in Fig. 1. The image is too faint for recording when it is viewed from 90 deg to the sheet. To resolve the vortex trajectory coordinates from the camera's viewing position, a grid board is carefully placed in the exact plane of the laser sheet before a test is begun. The video camera is then fixed in position, focus, and zoom, while the grid board image is recorded. Lines on the grid board are of known spacing, with the downstream (X) and vertical (Z) coordinates referenced to the rotor hub center. During data reduction the grid board image is superimposed on the laser sheet images produced during flow visualization. Thus, it is crucial that the camera remain undisturbed once the grid board is removed.

Forward Flight Results

A sample vortex trajectory obtained from flow visualization is shown in Fig. 2. The results correspond to the test arrangement shown in Fig. 1, at an advance ratio (μ) of 0.10. The geometric accuracy of the trajectory curve is estimated to be within 15 mm of the actual value, roughly corresponding to the core radius. As indicated in Fig. 2, the vortex core position is obtained as a function of blade azimuth angle. This is accomplished by adjusting the modulator deflection frequency so that the blade appears to advance slowly in the direction of rotor rotation. When reviewing the video tape, an image frame counter is initialized when the trailing edge of a particular blade tip passes through the laser sheet. At this instant, the coordinates of the newly emitted tip vortex are recorded, corresponding to approximately 190 deg of blade azimuth angle. As shown in Fig. 1, Ψ is measured from the rear airframe centerline to the blade quarter chord.

Subsequent vortex positions are noted along with the corresponding frame count until the desired number of rotor revolutions are complete. With the number of frames per rotor revolution known, the blade azimuth angle at any specified vortex position can be computed by a simple proportionality calculation. The accuracy in determining the vortex core position for a specified rotor azimuth angle is estimated to be ± 20 mm along the trajectory curve.

Since the vortex position is known as a function of time, its convective speed between two points can be estimated. For ex-

ample, Fig. 2 indicates that the blade rotates 90 deg while the tip vortex moves from $X/R = -1.0$ to $X/R = -0.83$. At the rotor speed of 2100 rpm, 90 deg of blade rotation corresponds to 0.00714 s. Thus, calculations show that, between the two points, the vortex core convects streamwise at 10.9 m/s. The freestream speed at $\mu = 0.10$ is 10.0 m/s, revealing that vortex convection in the X -direction is slightly greater than the freestream speed. This effect is caused by wake contraction.

Figure 2 shows that approximately 240 deg of blade rotation is required for a vortex emitted at $\Psi = 190$ deg to impact the airframe. Results from correlating flow visualization with the pressure signature measured on the airframe have been reported in Ref. 5.

Velocimetry techniques, when applied to rotors, often rely on the periodically repeating nature of the wake structure to obtain measurements near a vortex core. If a vortex core does not appear in the same spatial location for each turn of the rotor, the measured velocity pattern becomes smeared spatially, since the data are obtained over many revolutions. Such vortex jitter becomes apparent with this flow visualization technique as a fluctuating vortex position when the laser strobing is synchronized with the rotor.

By combining information from separate laser sheet positions, it is possible to construct a three-dimensional composite of the wake geometry. Careful and consistent measuring of Ψ is essential if the time variant characteristics of such a composite are desired.⁵

Conclusions

A strobed laser sheet technique for visualizing the periodic wake of a rotor has been developed that is suitable for studying a wide variety of situations common to rotorcraft. Coordinates of tip vortices can be resolved as a function of blade azimuth angle to a high degree of accuracy. Additionally, the convective velocities of vortex cores can be determined. Such a capability is useful in gathering data for the validation of prediction codes. This method provides a means for correlating vortex locations with measurements obtained from other instrumentation. Thus, it is extremely useful for gaining physical insights for interpreting periodic flow phenomena. The ability to observe vortices graphically in the rotor wake will also allow experimenters to assess problems that may arise from vortex jitter.

References

- Veret, C., "Flow Visualization by Light Sheet," *Flow Visualization III*, edited by W. J. Yang, Hemisphere, Washington DC, 1985, pp. 106-112.
- Porcar, R., Prenel, J., Diemunsch, G., Hamelin, P., "Visualizations by Means of Coherent Light Sheets; Applications to Various

Flows," *Flow Visualization III*, edited by W. J. Yang, Hemisphere, Washington DC, 1985, pp. 123-127.

³McGregor, I., "The Vapour-Screen Method of Flow Visualization," *Journal of Fluid Mechanics*, Vol. 11, Dec. 1961, pp. 481-511.

⁴Nelson, R. C., "The Use of Flow Visualization for Vortex Trajectory Mapping," *Flow Visualization III*, edited by W. J. Yang, Hemisphere, Washington DC, 1985.

⁵Brand, A. G., Komerath, N. M., McMahon, H. M., "Results from Laser Sheet Visualization of a Periodic Rotor Wake," AIAA Paper 88-0192, Jan. 1988.

⁶Brand, A. G., McMahon, H. M., Komerath, N. M., "Wind Tunnel Data From a Rotorwake/Airframe Interaction Study," School of Aerospace Engineering, Georgia Institute of Technology, Atlanta, GA. Contract No. DAAG29-82-K-0094, July 1986.

Thick Airfoil at Low Reynolds Number and High Incidence

S. Raghunathan,* J. R. Harrison,†
and B. D. Hawkins†

The Queen's University of Belfast
Belfast, Northern Ireland, United Kingdom

Nomenclature

c	= chord length
C_c	= chordwise force coefficient, $= C_l \sin \alpha - C_d \cos \alpha$
C_d	= drag coefficient, $= D/(\frac{1}{2}\rho V_\infty^2 c)$
C_l	= lift coefficient, $= L/(\frac{1}{2}\rho V_\infty^2 c)$
C_p	= pressure coefficient, $= (p - p_\infty)/(\frac{1}{2}\rho V_\infty^2)$
D	= drag force
F_c	= chordwise force
F_n	= force normal to chord
p	= static pressure on the airfoil
p_∞	= freestream static pressure
V_∞	= freestream velocity
x	= chordwise coordinate
α	= angle of incidence
ρ	= density of air

Introduction

AIR turbines used for wind and wave energy conversion have rotors with airfoil blades that operate over a wide range of Reynolds numbers and airflow incidence. Aerodynamics data on airfoils at low Reynolds numbers are available for some airfoils up to stall angle and for a few airfoils beyond stall (see, for example, Refs. 1-6). The understanding of the performance of a thick symmetrical airfoil at low Reynolds numbers and over a range of incidence of 0-90 deg is of particular importance to a Wells self-rectifying air turbine used for wave energy conversion.^{7,8} In a Wells turbine, the blades are set at a stagger angle of 90 deg. This Note presents some experimental data on an NACA 0021 airfoil at a blade chord Reynolds number of 2.6×10^5 and over a range of incidence of 0-90 deg. The results are compared with some of the data available on other airfoils and predictions by momentum theory.

Experiments

Isolated Airfoil

The experiments were conducted in a 0.84×1.145 -m closed-circuit low-speed wind tunnel that had a contraction ratio of 3 and a turbulence level in the test section of 0.2%. The model was an NACA 0021 airfoil section of 100-mm chord and spanning the width of the test section. The model was made of three sections of equal span with pressure orifices on the centerline of the midsection. There were 13 pressure orifices each on the upper and lower surfaces, one at the leading edge, and one at the trailing edge. Pressure measurements were made by a Scanivalve with a Druck transducer linked to an RML 380Z computer. Tests were performed at a freestream velocity of $V = 38$ m/s, which corresponded to a blade chord Reynolds number of 2.6×10^5 , and over a range of airflow incidences from 0-90 deg. Lift and drag values were calculated by integration of pressure distributions and were corrected for tunnel blockage effects. Oil-flow visualization studies were made for some selected test conditions.

Results and Discussion

The pressure distributions on the upper and lower surfaces of an NACA 0021 airfoil for the incidence range $0 \text{ deg} < \alpha < 20 \text{ deg}$ are shown in Figs. 1 and 2, respectively. Figure 3 shows a comparison of the present data for C_l for an NACA 0021 with those measured by Jacobs and Sherman² and Muller and Janson.⁵ The variations of C_l with incidence over the range of incidence $0 \text{ deg} < \alpha < 90 \text{ deg}$ are shown in Fig. 4. In this figure, the data for an NACA 0021 airfoil is compared with those of NACA 0015 and 0012 airfoils from Ref. 3 and predictions by momentum theory.⁴ The results for chordwise force coefficient C_c for several airfoils^{3,6} are compared with the present results in Fig. 5. It should be noted that the present data for C_c does not include skin-friction drag.

The C_p distribution on the upper surface (Fig. 1) shows that the trailing-edge pressure diverges significantly at $\alpha = 13 \text{ deg}$. As seen from the pressure distributions on the upper surface, there is a complete separation on the upper surface at the incidence of 13 deg. The C_p distribution on the upper surface continues to change with the increase in α after stall, but only gradually; for $\alpha > 26 \text{ deg}$ the C_p distributions on the upper sur-

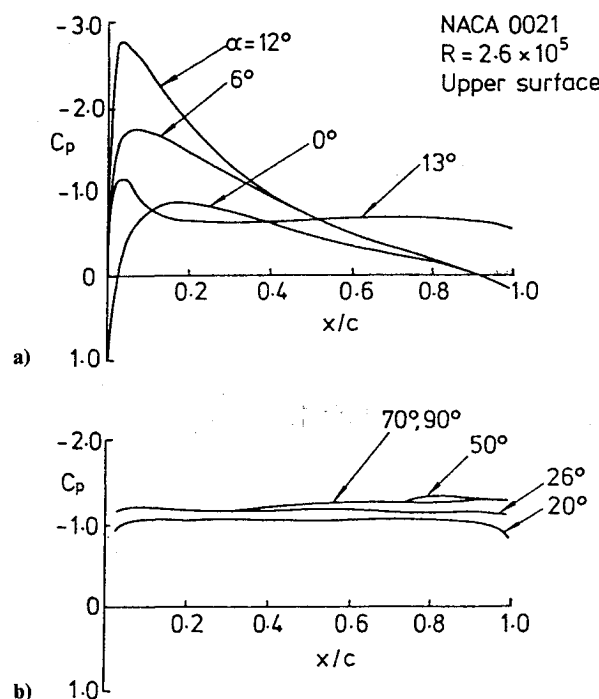


Fig. 1 Pressure distributions on the upper surface.

Received Oct. 2, 1987; revision received Oct. 27, 1987. Copyright © American Institute of Aeronautics and Astronautics, Inc., 1988. All rights reserved.

*Reader, Aeronautical Engineering.

†Graduate Student.